

Distribution Agreement

In presenting this thesis as a partial fulfillment of the requirements for a degree from Emory University, I hereby grant to Emory University and its agents the non-exclusive license to archive, make accessible, and display my thesis in whole or in part in all forms of media, now or hereafter now, including display on the World Wide Web. I understand that I may select some access restrictions as part of the online submission of this thesis. I retain all ownership rights to the copyright of the thesis. I also retain the right to use in future works (such as articles or books) all or part of this thesis.

Paavali Hannikainen

March 19, 2018

Molecular Characterization of A Growth-Factor Induced Glioblastoma Model

by

Paavali A. Hannikainen

Nicholas Boulis, MD

Adviser

Neuroscience and Behavioral Biology

Nicholas Boulis, MD

Adviser

Leah A. Roesch, PhD

Committee Member

John J. Stuhr, PhD

Committee Member

Mohib Tora

Non-Voting Committee Member

2018

Molecular Characterization of A Growth-Factor Induced Glioblastoma Model

By

Paavali A. Hannikainen

Nicholas Boulis, MD

Adviser

An abstract of
a thesis submitted to the Faculty of Emory College of Arts and Sciences
of Emory University in partial fulfillment
of the requirements of the degree of
Bachelor of Sciences with Honors

Neuroscience and Behavioral Biology

2018

Abstract

Molecular Characterization of A Growth-Factor Induced Glioblastoma Model

By Paavali A. Hannikainen

The development of therapeutics for the treatment for glioblastoma (GBM) have not been successful, with clinical trials failing by phase III. These failures in finding treatments can be attributed to the lack of an accurate preclinical animal model in which to test therapeutics. Specifically, orthotopic xenograft models do not recapitulate the heterogeneity, growth characteristics, and genetic make-up of human GBMs. Also, syngeneic models have issues with reproducibility and immunogenicity, where the model's immune system attacks the tumor. Thus, there is a need for a better GBM model. Research on GBM pathophysiology has shown that platelet-derived growth factor (PDGF) is a key protein for GBM tumorigenesis. A viral vector expressing PDGF was previously engineered and investigated. This viral vector can infect glial cells and cause the formation of tumors in the brain parenchyma with histological features that match the human GBM. However, it is unclear if the tumors also have similar molecular characteristics to human GBM. Tyrosine kinase receptors, specifically platelet-derived growth factor receptor-alpha (PDGFR- α) and epidermal growth factor receptor (EGFR), have been extensively investigated in human GBM, in addition to p53 and isocitrate dehydrogenase-1 (IDH-1). To validate this model as an accurate preclinical testing platform, the ability to replicate previous results and re-establish this model must be shown. In addition, further characterization of PDGF-induced tumor model must be completed through investigating PDGFR- α , EGFR, p53, and IDH-1 expression in PDGF-induced tumors. The results show successful reproduction of PDGF-induced tumors, as evidenced by staining showing typical histopathologic features of GBM, most notably pseudopalisading necrosis. In addition, characterization studies of PDGFR- α , EGFR, p53, and IDH-1 show that the model might not successfully recapitulate the molecular characteristics of GBM tumors.

Molecular Characterization of A Growth-Factor Induced Glioblastoma Model

By

Paavali A. Hannikainen

Nicholas Boulis, MD

Adviser

A thesis submitted to the Faculty of Emory College of Arts and Sciences
of Emory University in partial fulfillment
of the requirements of the degree of
Bachelor of Sciences with Honors

Neuroscience and Behavioral Biology

2018

Acknowledgments

I would like to thank Dr. Nicholas Boulis for allowing me to conduct my honors thesis project at his laboratory and supporting undergraduate involvement in the biomedical sciences. Also, thank you Mohib for your support and guidance throughout this project; this project would have never come to fruition without you. I would also like to thank the other undergraduates at the Boulis lab, specifically Yujin and Long, for their comradery and help with this project. Thank you Nathan Hardcastle for your technical guidance, and Dr. Claire-Anne Gutekunst and Kaavya Mandi for your help with troubleshooting immunohistochemistry. Thank you Dr. Peter Cannoll from Columbia University for providing us with the transgene constructs. Lastly, thank you Dr. Stuhr and Dr. Roesch for being part of my academic journey at Emory and my honors thesis committee.

Table of Contents

<u>Introduction</u>	1-6
Glioblastoma Multiforme and Failures in Treatment.....	1
Virally-Mediated Gene Delivery.....	2
Genetic Alterations in Human GBM.....	2
Platelet-Derived Growth Factor (PDGF) and Receptors.....	3
Epidermal Growth Factor Receptor (EGFR) in GBM.....	4
p53 in GBM.....	4
Isocitrate Dehydrogenase 1 (IDH-1) in GBM.....	5
Hypotheses.....	6
<u>Materials and Methods</u>	7-11
Retrovirus Packaging.....	7
Rat Surgeries.....	7
Brain Tissue Collection.....	8
Hematoxylin and Eosin Staining (H&E)	8
Moving from H&E Characterization to Immunohistochemical Characterization.....	9
Immunohistochemistry.....	9
Microscopy.....	10
<u>Results and Analysis</u>	12-14
Hematoxylin and Eosin Stain Analysis.....	12
Immunohistochemistry Analysis.....	12
Tumor Size and Viral Expression.....	14

<u>Discussion</u>	15-18
Re-establishing Virally-Induced PDGF Tumor Model.....	15
Tyrosine Kinase Receptors in PDGF-Induced Tumors.....	16
IDH-1 and p53 in PDGF-Induced Tumors.....	17
PDGF-Induced Tumor Model as a Preclinical Testing Platform.....	18
<u>Figures and Tables</u>	3, 19-26
Figure 1: Tyrosine Kinase Receptor Signaling Cascade.....	3
Figure 2: H&E Images of PDGF-Induced GBM in Rat Brain.....	19
Figure 3: Overexpression of PDGFR- α in PDGF-Induced Glioblastoma in Rat Brain.....	20
Figure 4: Decreased Expression of EGFR in PDGF-Induced Glioblastoma in Rat Brain.....	21
Figure 5: Decreased Expression of p53 in PDGF-Induced Glioblastoma in Rat Brain....	22
Figure 6: Inconclusive Regulation of IDH-1 in PDGF-Induced Glioblastoma in Rat Brain.....	23
Figure 7: Positive Immunohistochemistry Controls.....	24
Figure 8: DsRED Expression in PDGF-Induced Glioblastoma in Rat Brain.....	25
Table 1: Tumor Analysis Overview.....	26
<u>References</u>	27-30

Introduction:

Glioblastoma Multiforme and Failures in Treatment:

Approximately 30,000 patients in the United States are diagnosed with glioma every year, with glioblastoma multiforme (GBM) representing the most common and most malignant subtype (Holland, 2001; Stupp et al, 2005). GBM is a grade IV glioma classified by the World Health Organization (WHO) with a 5-year survival of less than 5%, and a median survival of 14.6 months. (Delgado-Lopez and Corrales-Garcia, 2016; Ostrom et al, 2014). This low survival rate can be attributed to the slow development of new therapeutics to treat GBM. Several potential treatments have shown promise in preclinical studies but none have passed phase III clinical trials and, as a result, there have been minimal changes in the standard of care (Seystahl et al, 2016).

The most plausible reason for the failure to develop novel therapeutics for the treatment of GBM is that current animal models are not able to recapitulate the histological features of human GBM. As an example, orthotopic xenograft models – including U87, U251, and U1242 animal models – are characterized by homogenous tumors and immunosuppressed animals; these factors poorly replicate GBM histopathological features and represent a failure in modeling GBM in animals (Jacobs et al, 2011). Furthermore syngeneic GBM models, including CL261, C6, and 9L animal models, are formed through the application of a carcinogens to create a tumor cell line that has an intact immune system, unlike xenograft models. They still fail to recapitulate histopathologic features of human GBM as they have problems with immunogenicity (Chen et al, 2013). Even though current models show proof-of-concept, these features of current GBM models limit the utility of the models as pre-clinical therapeutic testing platforms. To make therapeutic progress in the treatment of GBM, an accurate animal model which develops clinically relevant histological and genetic characteristics of the disease is necessary.

Virally-Mediated Gene Delivery:

Advances in virally-mediated gene delivery provide an opportunity to understand the pathophysiology of GBM, allowing for the examination of genetic changes found in human GBM without the limiting features found in xenograft and syngeneic models. Gene delivery might permit the generation of a potentially superior GBM model systems with the ability to recapitulate the histopathological features of GBM, allowing for the development of an accurate therapeutic testing platform.

A model showing this kind of promise is a virally-induced model that expresses platelet-derived growth factor (PDGF) in glial cells. Injection of a retrovirus that upregulates PDGF in the rat brain parenchyma results in a large, infiltrative intracranial tumors with hallmark histological features of GBM within 14 days of injection. These tumors resemble GBM, evidenced by previously published low-resolution MRI images and staining for limited histopathologic markers, such as glial progenitor markers Olig2, and Ki67 (Assanah et al, 2006). However, a large deficit of PDGF induced GBM models is the lack of robust molecular and genetic characterization. These characterization analyses are important in order to establish that the model is accurately replicating the human GBM equivalent, and as a result establish the model as an accurate platform for testing therapeutics (Ceccarelli et al, 2016; Appin et al, 2015).

Genetic Alterations in Human GBM:

Frequently encountered alterations in genes in human GBM have been identified, and these include amplification of platelet-derived growth factor receptor-alpha (PDGFR- α) and epidermal growth factor receptor (EGFR), in addition to mutations of p53 tumor suppressor protein and isocitrate dehydrogenase 1 (IDH-1) enzyme (Nazarenko et al, 2012; Lee et al, 2013). Specifically, immunohistochemical overexpression of EGFR, p53, and IDH-1 in 150 human GBMs were

observed in 62.6%, 49.3%, and 11.1% of samples, respectively (Lee et al, 2013). In order for the virally-induced PDGF model to be an accurate model of the human GBM equivalent, PDGFR- α , EGFR, p53, and IDH-1 alterations should be present in the PDGF model.

Platelet-Derived Growth Factor (PDGF) and Receptors:

PDGF is a dimeric protein consisting of five isoforms, functioning as a stimulus for cell growth, survival, and motility in both embryonic and mature cells (Heldin and Westermark, 1999; Andrae et al, 2008). PDGF overexpression has been implicated in the development tumors and non-malignant diseases, as PDGF stimulates excessive cell proliferation; in fact, many tumor treatments target PDGF with antagonists (Heldin, 2014).

PDGF exerts its function through binding to α - and β -tyrosine kinase receptors (TKRs): PDGFR- α and PDGFR- β . Binding of PDGF to either TKR results in phosphorylation and activation of its receptors. This activation and subsequent cell signaling cascade in turn results in cell proliferation, migration, and survival, as represented in Figure 1 (Krakstad and Chekenya, 2010).

PDGF overexpression is a major factor in the development of GBM as well (Nazarenko et al, 2012). PDGF overexpression results in over-activation of PDGF receptor signaling pathway, resulting in sustained growth and formation of tumor. Not only PDGF has been shown to be

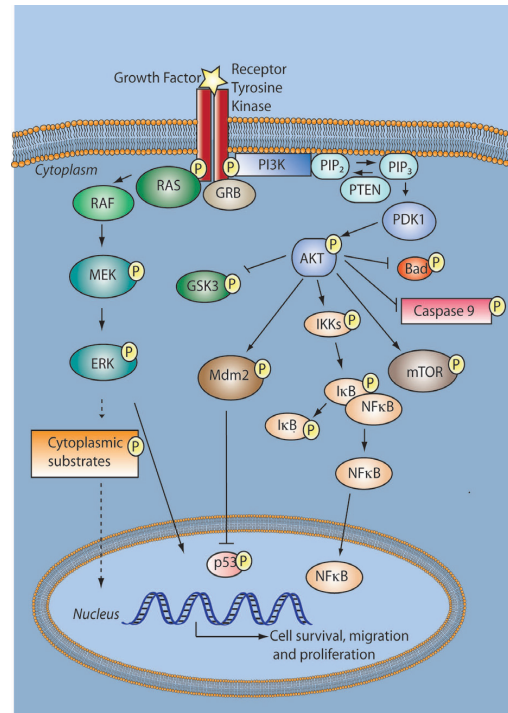


Figure 1: Tyrosine kinase receptor signaling cascade, with activation through growth factor ligand binding. Includes PDGFRs and EGFRs in GBM (Krakstad and Chekenya, 2010)

Author permission for reproduction obtained, in addition to image being part of the Creative Commons Attribution License.

upregulated in gliomas, but also its receptors, including PDGFR- α (Brennan et al, 2013). This suggests that autocrine and paracrine PDGF signaling might play a role in growth and progression of GBM (Hermanson et al, 1992; Di Rocco et al, 1998). For the PDGF-induced tumor model to replicate the human GBM equivalent accurately, tumors with overexpression of PDGFR- α are expected to be observed.

Epidermal Growth Factor Receptor (EGFR) in GBM

Another TKR implicated in GBM, is EGFR, which has been found to be upregulated in approximately 60% of GBMs (Lee et al, 2013). Ligand binding to EGFR and subsequent EGFR activation results in a similar intracellular signaling cascade as PDGF, seen in Figure 1 (Krakstad and Chekenya, 2010). Similarly to PDGF, EGFR has been used frequently as an antagonistic target for the treatment of GBM. Many different mechanisms have been implicated in the overexpression of EGFR, including increased receptor protein levels, malfunction in receptor degradation, and crosstalk with other receptors, such as PDGFRs (Xu et al, 2016). Similarly to PDGFR- α , PDGF-induced tumors would be expected to also overexpress EGFR.

p53 in GBM

p53 is a tumor suppressor protein and functions as a transcription factor, regulating cell growth, apoptosis, and DNA repair (Vogelstein et al, 2000). Alterations the p53 gene is a distinct feature in GBMs (Ohgaki, 2005). Specifically, p53 has been found to be involved in disease progression of GBM. Alterations of the p53 gene in GBM include mutation or allelic loss of 17p13.1 (Chen et al, 1999), with 49.3% of 150 patient samples of GBM showing immunohistochemical over-expression of p53 (Lee et al, 2013). PDGF-induced tumors would be expected to also overexpress p53.

Isocitrate Dehydrogenase 1 (IDH-1) in GBM

IDH-1 is a protein found throughout the cell, including cytoplasm, peroxisomes and the endoplasmic reticulum. IDH-1 catalyzes the conversion of isocitrate into α -ketoglutarate (Koshland et al, 1985; Geisbrecht et al, 1999; Margittai and Banhegyi, 2008). IDH-1 mutations have been used to define the difference between primary and secondary GBMs (Ohgaki and Kleihues, 2007). Primary GBMs represent approximately 90% of all GBMs and develop rapidly in elderly patients, with no previous evidence of a less malignant lesion. Secondary GBMs are found in younger patients and have better prognosis than primary GBMs.

Although primary GBMs do not present signs of IDH-1 mutations, 70-80% of secondary GBMs have somatic mutations of IDH-1 (Bleeker et al, 2010; Guo et al, 2011; Alexander et al, 2011). No clear mechanism of IDH-1 mutations in tumors has been established, but mutations might result in epigenetic changes or decreased production of NADPH (Alexander et al, 2011). Consequently, IDH-1 mutations have been shown to be associated with increased survival of patients with GBM. Through decreased production of NADPH, GBM tumor cells might be more susceptible to radiation and irradiation treatments (Baldewpersad et al, 2013; Chen et al, 2016). Investigation of IDH-1 mutations in PDGF-induced tumors is needed to understand the cellular changes that occur in PDGF-induced tumors, and subtype tumors into primary or secondary GBM.

Hypotheses

1. Virally-induced PDGF tumors will be able to be induced in the rat forceps minor of the corpus callosum within 14 days of injection, with H&E staining demonstrating histopathological characteristics of human GBM, including pseudopalisading necrosis, increased vascularity, nuclear atypia, cortical invasion, and mass effect.

2. Virally-induced PDGF tumors in the rat brain resemble expression of human GBM equivalent, as seen by increased expression of PDGFR- α , EGFR, p53, and alterations of IDH-1 enzyme in IHC staining.

Materials and Methods:

Retrovirus Packaging:

A retrovirus was used to overexpress PDGF and was engineered with an out-sourced company; PDGF-IRES-DsRED was packaged into a pQCXIX retroviral vector (Clontech, Catalog Number 631515). The vector identity was confirmed by sequencing and a titer of 4.09×10^8 TU/ml was obtained (ViGene Biosciences).

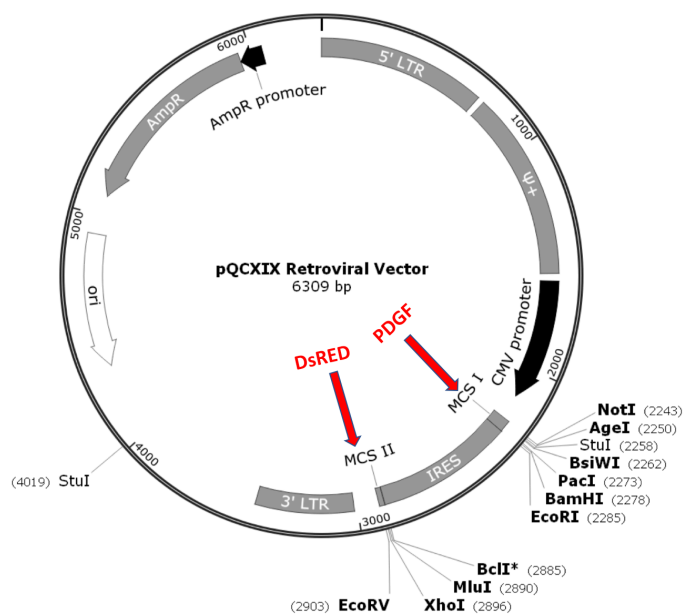


Figure 1: Location of DsRED and PDGF in Packaged Retrovirus

Rat Surgeries:

An intraparenchymal injection protocol was used in a total of 13 Sprague Dawley rats (Charles River). The animals were anesthetized with isoflurane, incision made midline in the scalp, stereotactic guidance used for burr hole placement, and 5 μ l injection of virus with an injection rate of 0.5 μ l/min was injected into the forceps minor of the corpus callosum (stereotactic coordinates relative to bregma: 2 mm lateral, 2.5mm rostral, 3.5 mm deep). The needle was removed and the scalp sutured closed. Animals were sacrificed at different time points based on signs of morbidity (15, 16, and 17 days post-injection), although two animals were found dead

before being able to be sacrificed. Signs of morbidity included weight loss, seizures, posturing, periorbital hemorrhage, and perforin stains around the eyes.

Brain Tissue Collection:

The first pilot study consisted of injection of the virus in five rats, meanwhile the second study consisted of eight rats. The animals from the pilot study were fixed with cardiac perfusion using 4% paraformaldehyde (PFA), brains excised, and frozen in -80°C . The five brains from the pilot study were cut using a cryostat into $20\ \mu\text{m}$ sections directly onto microscope slides and stored in -20°C . Meanwhile in the second study, four brains were excised and fresh-frozen, and saved for western blot analysis and genome sequencing. The other four brains were fixed with cardiac perfusion using 4% PFA, brains excised, and frozen in -80°C . Three of the brains in the second study were cut into $20\ \mu\text{m}$ sections directly onto microscope slides, meanwhile one brain was cut into $40\ \mu\text{m}$ sections. This was necessary due to the large size of the tumor observed during cutting, resulting in the brain being fragile and no slides with an intact tumor were able to be collected using $20\ \mu\text{m}$ sections. Doubling the thickness of brain sections allowed for the preservation of tumor tissue. Microscope slides with brain sections were stored in -20°C .

Hematoxylin and Eosin Staining (H&E)

The sections from nine brains underwent H&E staining with subsequent assessment using World Health Organization (WHO) glioma grading. Grading included assessment for the presence of pseudopalisading necrosis, vascularity, nuclear atypia, cortical invasion, and mass effect. Out of 9 brains that were sectioned, 6 were confirmed to have a tumor. Specifically, in the pilot study three out of five brains had a tumor, and three out of four brains were confirmed to have tumor in the second study.

Moving from H&E Characterization to Immunohistochemical Characterization

One of the animals was found dead during the pilot study and H&E analysis was completed to confirm the presence of a tumor, but not further analysis was completed on the tumor due to improper fixation as the animal had passed away and no cardiac perfusion was able to be completed. In addition, one brain tumor was particularly small and only H&E staining could be completed on the brain due to lack of multiple microscope slides with tumor tissue. One of the sectioned brains also had poor adherence to the microscope slides and significant number of wrinkles on slides. As a result, only three brains that were confirmed to have tumor went through immunohistochemistry (IHC) staining to investigate cellular changes in PDGF-induced tumors.

Immunohistochemistry:

Immunohistochemical protocol began with antigen retrieval using citrate buffer at pH of 6.0 overnight in an oven at 70°C rather than boiling water bath to preserve tissue. In addition, instead of using Phosphate Buffered Saline (PBS), Tris-Buffered Saline (TBS) was used to wash and permeabilize tissue and mix antibodies with, as the phosphate in PBS might have interfered with phosphate conjugated antibodies. The primary antibodies used were anti-IDH-1 (abcam, ab214803, 1:100 concentration), anti-PDGFR- α (abcam, ab5460, 1:50 concentration), anti-EGFR (abcam, ab52894, 1:100 concentration), and anti-p53 (abcam, ab1431, 1:50 concentration). The secondary bodies used were goat anti-rabbit immunoglobulin G (IgG) heavy and light (H&L) chain (abcam, ab6721, 1:1000 concentration) and a biotin conjugated antibody goat anti-rabbit IgG H&L (Jackson Laboratories, 111-065-003, 1:250 concentration). With the AffiniPure antibody, a tertiary antibody was used, which consisted of avidin/biotin ABC complex in the VECTASTAIN® ABC-horseradish peroxidase (HRP) kit (Vector Laboratories, PK-6100). Amplification of signal was completed using the biotin conjugated secondary antibody and avidin/biotin tertiary antibody after

not being able to obtain a signal using a standard secondary antibody. At the end of the protocol, color change was obtained using 3,3'-diaminobenzidine (DAB) peroxidase substrate kit (Vector Laboratories, SK-4100) for five minutes.

The recommended positive controls by abcam were obtained for anti-EGFR, anti-PDGFR- α , and anti-IDH-1. These controls were stained using the same protocol as brain slides with tumors. The positive controls included A-431 cell slides fixed in 4% PFA (ProSci, 10126-886) for EGFR detection, 3T3/NIH cell slides fixed in 4% PFA (ProSci, 10126-910) for PDGFR- α detection, and HeLa cell slides fixed in 4% PFA (ProSci, 10126-884) for IDH-1 detection. For anti-p53, the recommended positive control by abcam was either rat bone marrow cells or UV treated HeLa cells. These cell slides were not able to be obtained, but instead human bone marrow cells were acquired, which were K-562 cell slides fixed in 4% PFA (GeneTex, 89346-790).

Microscopy:

Imaging of H&E stains and IHC stains were performed using Nikon Eclipse E400 microscope and Nikon DS-Fi1 camera. H&E images were acquired using bright-field microscopy and Nikon NIS-Elements software. For whole brain images of H&E and IHC stains, 2X objective was used to capture images, saved as TIFF files, and stitched together using Adobe Photoshop. Same procedure without stitching was followed when using 4X and 10X objective for close-up images of H&E and 40X objective for close-up images of IHC. Control samples were imaged using 20X objective. All parameters of the camera were kept constant when imaging IHC in the controls and tumor, with exposure kept at 67ms.

For DsRED detection in tumor, fluorescence microscopy was used with the same Nikon Eclipse E400 microscope, but Nikon DS-Qi1Mc camera was used instead. TRITC filter and 4X

objective was used and images were acquired using the same Nikon NIS-Elements software and saved as TIFF files. Adobe Photoshop was used to outline tumor area for visualization purposes.

Results and Analysis:

Hematoxylin and Eosin Stain Analysis:

In Figure 2: H&E Images of PDGF-Induced GBM in Rat Brain, histopathological features of GBM can be observed. Specifically, nuclear atypia with increased dark purple hematoxylin stain can be observed in both images with tumor. Because hematoxylin binds to nucleic acids, nuclear atypia can be observed as darkened stain in the slide. In addition, mass effect in both images with growing mass can be observed; in panel B, it is possible to observe the growing mass pushing the surrounding tissue, resulting in the tumor containing hemisphere looking enlarged in the H&E stained section. In addition, increased vascularity can be observed in both panels with increased number of vessels and increased vessel diameter. Furthermore, cortical invasion can be detected in panel B, with tumor cells invading the right and top corners in the brain section. Lastly, pseudopalisading necrosis can be observed in panel B, with the 10X image showing necrotic foci in the middle. This foci is surrounded by pseudopalisading cells, which are unique to malignant gliomas, specifically WHO grade IV glioblastoma, and is prognostic feature utilized by clinicians in the diagnosis of GBM (Rong et al, 2006).

Immunohistochemistry Analysis:

Figure 3: Overexpression of PDGFR- α in PDGF-Induced Glioblastoma in Rat Brain, shows overexpression of PDGFR- α as indicated by increased number of darkened cells in tumor when compared to the contralateral non-tumor hemisphere. In addition, appropriately comparing to Figure 7: Positive Immunohistochemical Controls, dark cells positive for PDGFR- α can be observed in panel A, supporting that PDGFR- α was detected in tumor tissue through the utilized IHC protocol. PDGFR- α overexpression was observed in all three brain tumors that were stained for PDGFR- α , as reported in Table 1: Tumor Analysis Overview.

Figure 4: Decreased Expression of EGFR in PDGF-Induced Glioblastoma in Rat Brain, shows less expression of EGFR in tumors as cells with minimal stain can be observed, and the overall stain in the tumor is less dark than the contralateral hemisphere with no tumor. In addition, looking at Figure 7: Positive Immunohistochemical Controls, dark cells positive for EGFR can also be observed in panel B, supporting that EGFR would have been detected in the tumor if it was being expressed. Decreased expression of EGFR was observed in all three brain tumors that were stained for EGFR, as reported in Table 1: Tumor Analysis Overview.

Figure 5: Decreased Expression of p53 in PDGF-Induced Glioblastoma in Rat Brain, shows less expression of p53 in tumor as the stain is less dark in the tumor side of the tissue when compared to the contralateral hemisphere with no tumor. The human bone marrow anti-p53 control did not turn a positive signal, with no ability to confirm that the IHC protocol was appropriate for p53 detection. This decreases the reliability of drawing conclusions from these results, but decreased stain was still able to be observed in all three brain tumors when compared to the contralateral hemisphere with no tumor, as reported in Table 1: Tumor Analysis Overview.

Figure 6: Inconclusive Regulation of IDH-1 in PDGF-Induced Glioblastoma in Rat Brain shows two panels, with increased dark cells in panel A with PDGF-induced tumor in one brain, meanwhile no difference in the stain in panel B with PDGF-induced tumor in a different brain. As seen in Table 1: Tumor Analysis Overview, two brains showed no difference in stain, which panel B is representative of, meanwhile just one brain, panel A, showed increased number of dark cells. Looking at Figure 7: Positive Immunohistochemical Controls, dark cells positive for IDH-1 can be observed in panel C, supporting that IDH-1 was stained in appropriately with the utilized protocol.

Tumor Size and Viral Expression

Of the six confirmed tumors with H&E staining, the average tumor length as measured through sectioning was 1053 μm , and the average width through imaging was 2702 μm , as reported in Table 1: Tumor Analysis Overview. In addition, viral expression was confirmed in tumors through DsRED imaging, as seen in Figure 8: DsRED Expression in Tumor. The engineered virus along with PDGF expresses DsRED, so viral expression of PDGF can be confirmed through observing DsRED light-emission.

Discussion:

Re-establishing Virally-Induced PDGF Tumor Model:

The results show successful replication and establishment of a virally-induced PDGF tumor model at the Boulis laboratory. This is evident by H&E staining showing typical histopathological features of glioblastoma including increased vascularity, nuclear atypia, cortical invasion, mass effect, and most notably pseudopalisading necrosis, marking the tumor to be WHO grade IV glioma. In addition, DsRED expression shows that the tumor cells express PDGF successfully, and the fluorescence across the tumor shows that the virus has infected glial cells across the tumor. Lastly, the significant size of the tumor with evident mass effect within 15-17 days of injection shows the invasive nature of the tumor, similar to human GBM. All of these characteristics point to the ability to replicate PDGF-induced tumor models, a feature necessary to establish this model as a proper preclinical treatment platform. In addition, these histopathological features all point to grade IV glioma, as previously established by Assanah et al, 2006.

On the other hand, only six out of nine animals developed tumors as seen in Table 1: Brain Analysis Overview and could point to issues with the tumor model. This can be attributed to the introduction of stereotactic injection protocol specific to the forceps minor of the corpus callosum in the laboratory. This area is part of the subcortical white matter and contains one of the largest numbers of glial progenitors in the brain, which the virus exclusively infects (Dawson et al, 2003). Compared to the pilot study, a larger proportion of animals developed tumors in the second study, as determined by H&E staining; specifically, 75% of animals in second study showed signs of tumors compared to 60% in pilot study. This represents an improvement in the delivery of virus to the forceps minor of the corpus callosum, as missing this subcortical white matter might result in no infection of glial cells and no tumor development.

Tyrosine Kinase Receptors in PDGF-Induced Tumors:

Further characterization was completed to understand the cellular changes that occur in PDGF-induced tumors. This included examining commonly amplified TKRs in GBM through IHC, specifically EGFR and PDGFR- α . The results show that as hypothesized, PDGFR- α was upregulated in PDGF-induced tumors. PDGFR- α overexpression has been previously reported in 10-15% of GBMs (Brennan et al, 2013), with Assanah et al, 2006 previously staining for this marker and showing expression of PDGFR- α in PDGF-induced tumors. Furthermore, along with PDGF expression in gliomas, its receptors have been shown to be subsequently expressed as well, providing evidence for autocrine and/or paracrine PDGF signaling (Hermanson et al. 1992; Westermarck et al, 1995; Di Rocco et al, 1998). PDGF overexpression in GBMs might directly increase PDGFR- α expression in the same or nearby cells, resulting in the observed PDGFR- α overexpression. These results support the hypothesis that PDGF-induced tumors model the human GBM equivalent.

On the other hand, decreased expression of EGFR was observed in PDGF-induced tumors. EGFR is one of the most well studied receptors in GBM, with overexpression being reported in more than 60% of GBMs; more overexpression than any other reported receptor in GBM (Lee et al, 2013). Surprisingly, PDGF-induced tumors showed decreased expression of EGFR, with no previous literature – to knowledge – reporting on decreased expression of EGFR in GBM. Decreased expression of EGFR might be a way for the tumor cell to evade sustained growth, as EGFR expression is implicated in sustained tumor growth. This result goes contrary the hypothesis and shows a possibly limiting aspect of PDGF-inducing tumors as preclinical models of GBM.

IDH-1 and p53 in PDGF-Induced Tumors

In addition to looking at TKRs, other commonly reported cellular changes in GBM were examined, including IDH-1 enzyme and p53 protein expression. The IDH-1 analysis showed no definitive conclusion as to whether IDH-1 alterations are present in PDGF-induced tumors, although majority of the tumors analyzed showed no alterations. Assuming that there are no IDH-1 alterations present in PDGF-induced tumors, primary GBM subtype might be implicated as they have no signs of IDH-1 mutations, unlike majority of secondary GBMs (Bleeker et al, 2010; Guo et al, 2011; Alexander et al, 2011). Still, more extensive analyses must be conducted to better understand IDH-1 expression in PDGF-induced tumors, such as quantitative western blot analysis and genome sequencing of tumors.

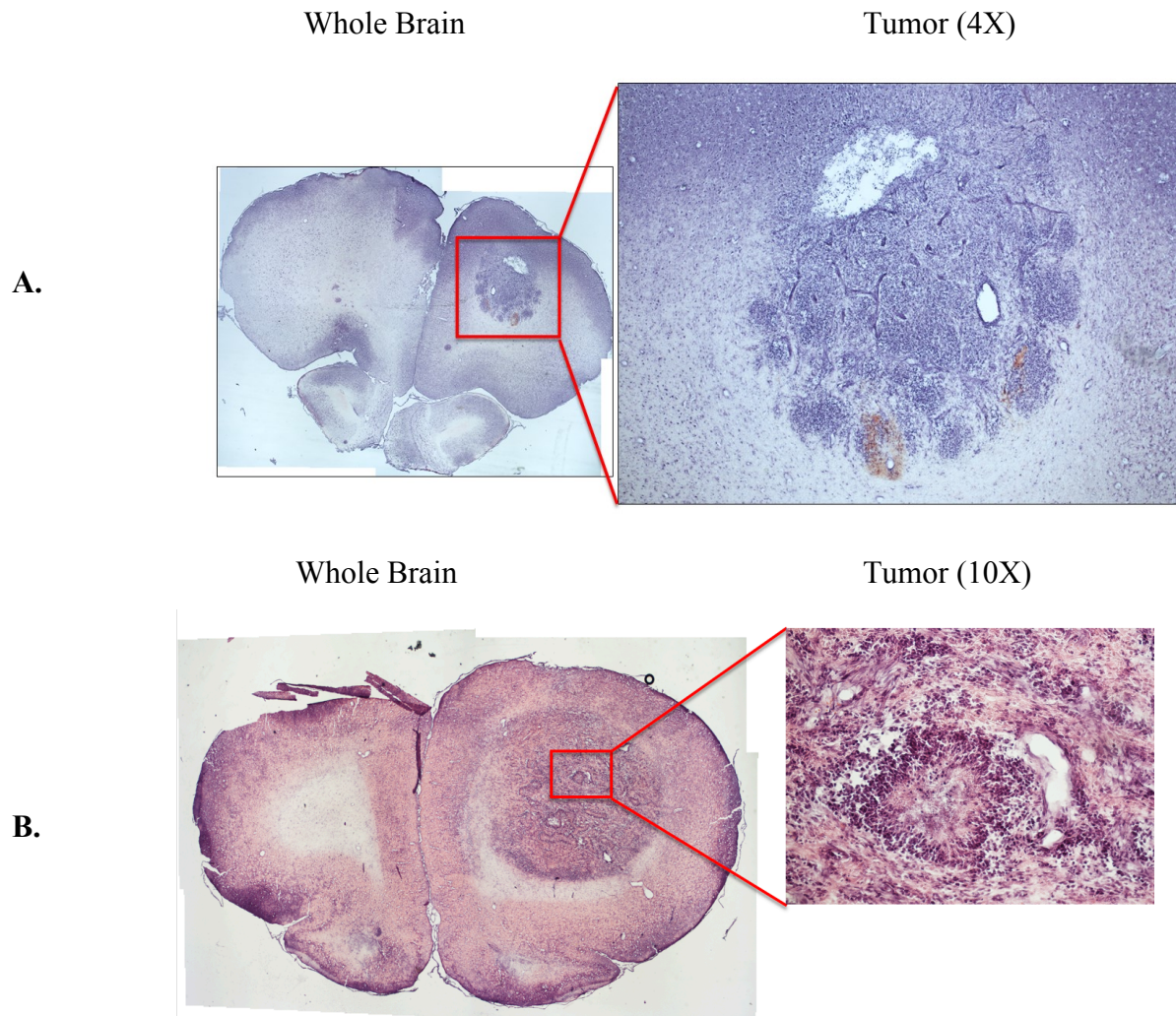
The results suggest that decreased expression of p53 might occur in PDGF-induced tumors, although the IHC stain for anti-p53 was not able to be confirmed with an appropriate positive control. This goes contrary to the hypothesis that p53 would be overexpressed in PDGF-induced tumors. Overexpression of p53 is observed in human GBM due to loss of heterozygosity, resulting in genomic instability and subsequent accumulation of p53 in the nucleus and cytoplasm of cells. In the case of homozygous deletion of p53, decreased expression of p53 can be observed in human GBMs, with 18% of human GBM samples in a study characterizing p53 expression having no p53 expression (Nagpal et al, 2006). Although this goes contrary to the hypothesis with overexpression of p53 being more common than loss of p53 expression in GBM, total loss of p53 has been detected in GBM samples. As a result, decreased expression of p53 could be expected in PDGF-induced tumors resembling human GBM.

PDGF-Induced Tumor Model as a Preclinical Testing Platform:

It has been argued that EGFR and p53 mutations are mutually exclusive in the development of GBM and represent two different genetic pathways in gliomagenesis. Primary GBMs have EGFR overexpression, with little evidence for p53 or IDH-1 alterations. On the other hand, secondary GBMs have p53 and IDH-1 mutations and no EGFR alterations (Ohgaki et al, 2013). Based on preliminary characterization of four cellular markers through IHC, it is not possible to classify PDGF-induced tumors into either primary or secondary glioblastoma. If decreased expression of p53 is observed in PDGF-induced tumors, it would not be expected to observe mutations of EGFR as well. Contrary to this paradigm, PDGF-induced tumors showed decreased expression of both p53 and EGFR. Furthermore, decreased EGFR expression in human GBM has not been reported, to knowledge, suggesting that PDGF-induced tumor models might not be reliable preclinical testing platforms for human GBM. Still, only a few cellular markers were characterized through IHC, and PDGFR- α upregulation was still observed in PDGF-induced tumors, as seen in human GBM. Furthermore, an appropriate p53 positive control needs to be added to confirm that the IHC protocol utilized was detecting p53 properly, such as UV treated HeLa cells. Also, the H&E analysis shows characteristic features of human GBM, most significantly pseudopalisading necrosis that is characteristic of grade IV glioma: GBM. Based on this evidence, it is hard to conclude whether PDGF-induced tumors are accurately representing human GBM. Further investigations needs to be completed, including more quantitative methods of cellular changes: western blot analysis, in addition to genome sequencing to see at the genetic level what is happening inside virally-induced PDGF tumors.

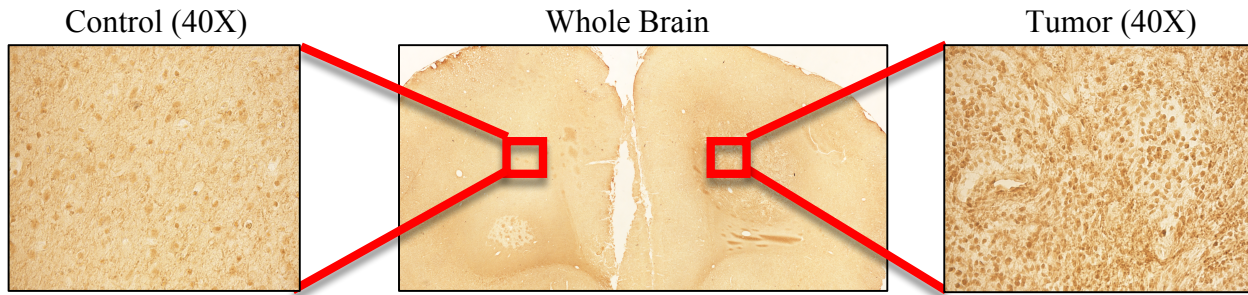
Figures and Tables:

Figure 2: H&E Images of PDGF-Induced GBM in Rat Brain



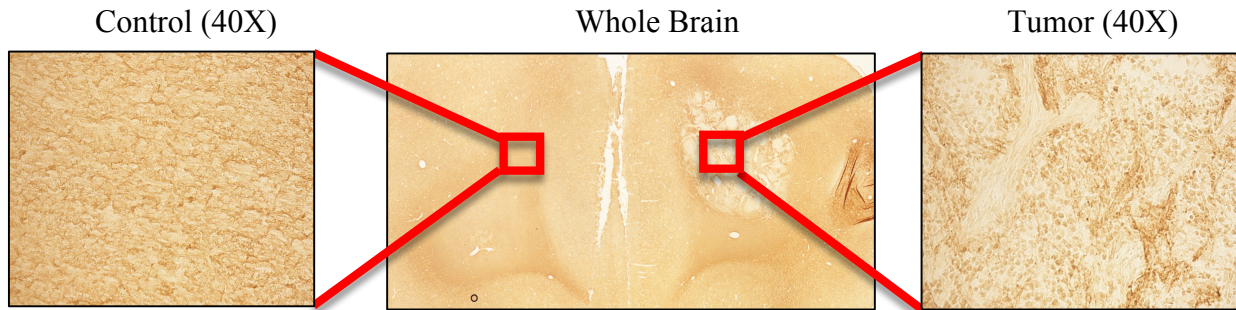
Rats were sacrificed 15-17 days post-injection of retroviral PDGF-DsRED. Rats underwent cardiac perfusion of 4% PFA, followed by brain harvesting and sectioning. Sections were stained with H&E using standard staining protocol. Analysis of brain sections show pseudopalisading necrosis (**B**), increased vascularity (**A, B**), nuclear atypia (**A, B**), cortical invasion (**B**), and mass effect (**A, B**), all consistent with GBM histopathology.

Figure 3: Overexpression of PDGFR- α in PDGF-Induced Glioblastoma in Rat Brain



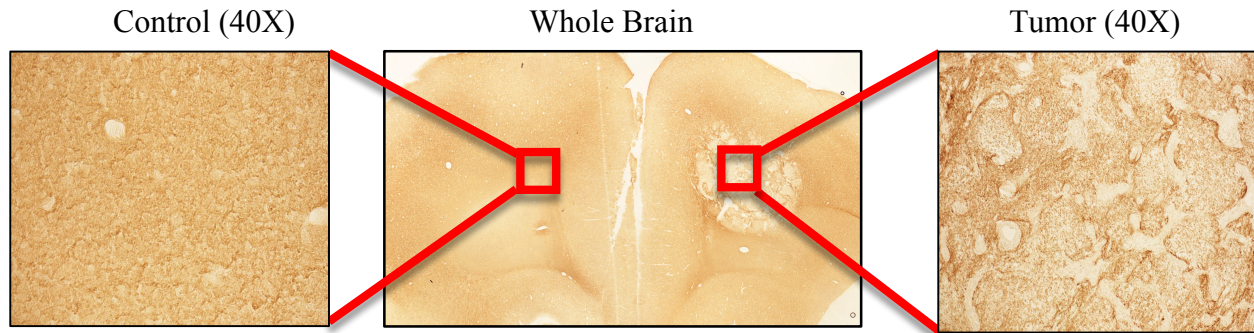
Three brains with confirmed tumors from H&E staining were stained for anti-PDGFR- α (1:50 concentration) using immunohistochemistry. Analysis of brain sections shows overexpression of PDGFR- α , as evidenced by increased number of dark cells in tumor side of brain section.

Figure 4: Decreased Expression of EGFR in PDGF-Induced Glioblastoma in Rat Brain



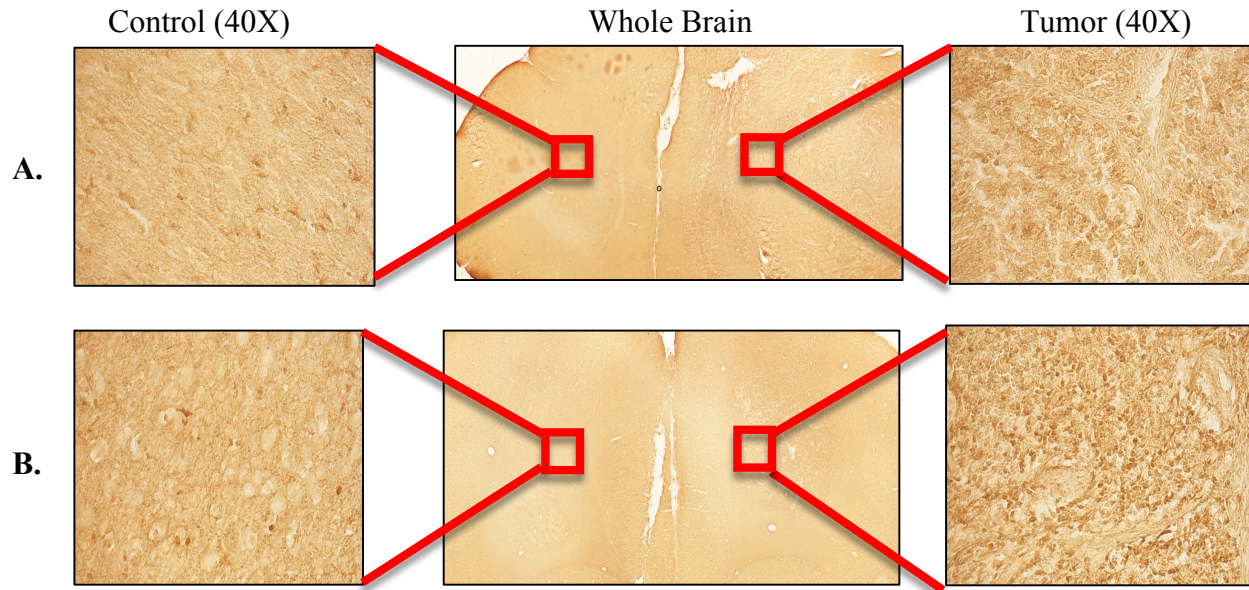
Three brains with confirmed tumors from H&E staining were stained for EGFR (1:100 concentration) using immunohistochemistry. Analysis of brain sections shows decreased expression of EGFR, as evidenced by decreased DAB staining intensity and cells with minimal stain can be observed in the tumor side of brain section.

Figure 5: Decreased Expression of p53 in PDGF-Induced Glioblastoma in Rat Brain



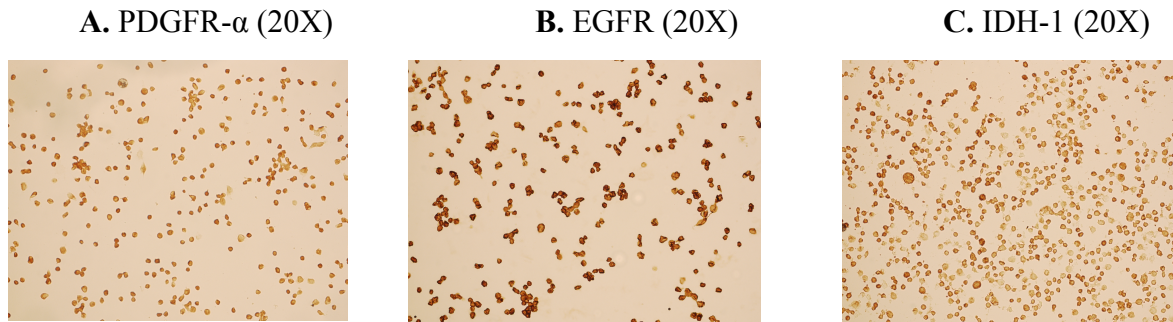
Three brains with confirmed tumors from H&E staining were stained for anti-p53 (1:50 concentration) using immunohistochemistry. Analysis of brain sections shows decreased expression of p53, as evidenced by decreased stain in tumor side of tissue.

Figure 6: Inconclusive Regulation of IDH-1 in PDGF-Induced Glioblastoma in Rat Brain



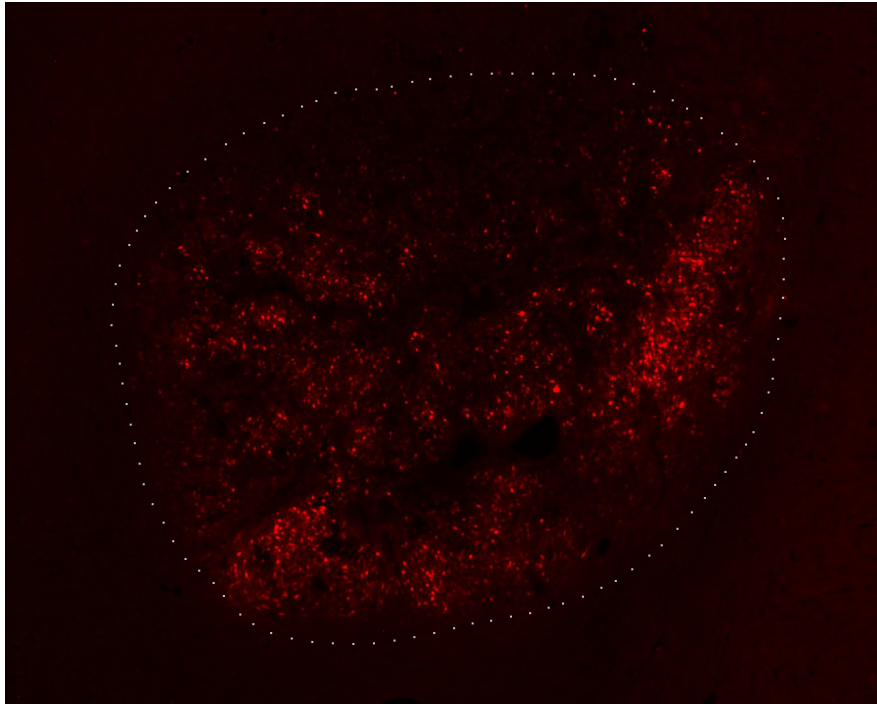
Three brains with confirmed tumors from H&E staining were stained for anti-IDH-1 (1:100 concentration) using immunohistochemistry. Analysis of brain sections shows inconclusive regulation of IDH-1, as evidenced by increased dark cells in one brain (A.) with PDGF-induced tumor, meanwhile no difference in the stain in two brain tumors (B.).

Figure 7: Positive Immunohistochemistry Controls



A. 3T3/NIH Cell Slide was stained for anti-PDGFR- α (abcam, ab5460, 1:50 concentration). **B.** A-431 Cell Slides was stained for anti-EGFR (abcam, ab52894, 1:100). **C.** HeLa Cell Slide was stained for anti-IDH-1 (abcam, ab214803, 1:100 concentration). Primary antibody incubation was followed with a biotin conjugated secondary antibody, and a tertiary antibody with avidin/biotin complex for signal amplification. Signal was obtained using DAB peroxidase, and antigen retrieval in citrate buffer was completed prior to IHC staining.

Figure 8: DsRED Expression in PDGF-Induced Glioblastoma in Rat Brain



Nikon Eclipse E400 microscope with TRITC filter and 4X objective with Nikon DS-Qi1Mc camera was used to detect DsRED expression in a 20 μm section of a PDGF-induced tumor. Adobe Photoshop was used to outline tumor area. DsRED expression is seen across the tumor, showing continuous expression of PDGF in proliferating cells.

Table 1: Tumor Analysis Overview

Brain	Size:		Immunohistochemistry:				Notes:
	Tumor length (µm)	Tumor width (µm)	IDH-1	PDGFR- α	p53	EGFR	
1 ^a	420	1482	N/A	N/A	N/A	N/A	Animal found dead
2 ^a	800	2961	+	+	-	-	
3 ^a	2660	3766	N/A	N/A	N/A	N/A	Poor adherence to slide, significant wrinkles
4 ^a	No tumor	N/A	N/A	N/A	N/A	N/A	
5 ^a	No tumor	N/A	N/A	N/A	N/A	N/A	
6 ^b	140	824	N/A	N/A	N/A	N/A	Not enough tissue for IHC
7 ^b	1100	3609	0	+	-	-	
8 ^b	1200	3575	0	+	-	-	40 µm sections
9 ^b	No tumor	N/A	N/A	N/A	N/A	N/A	
Mean:	1053	2702					

Tumor length was measured by H&E staining and finding through this method the first and last section with tumor. ImageJ was used to measure tumor width in the middle slide of tumor by measuring pixels and obtaining image calibration from Nikon Elements imaging software for each image. With regard to immunohistochemistry, 0 refers to no change in expression of marker, + refers to overexpression of marker, and – refers to decreased expression of marker when comparing tumor to no tumor hemisphere. Exclusion criteria for not completing immunohistochemistry included not having enough tissue with tumor, if animal was found dead prior to cardiac perfusion, and poor tissue morphology on microscope slide. In the “Brain” column, a refers to pilot study and b refers to second study.

References:

- Alexander BM, Mehta MP (2011) Role of isocitrate dehydrogenase in glioma. *Expert Rev Neurother* 11:1399–1409.
- Andrae J, Gallini R, Betsholtz C (2008) Role of platelet-derived growth factors in physiology and medicine. *Genes Dev* 22:1276–1312.
- Appin CL, Brat DJ (2015) Molecular pathways in gliomagenesis and their relevance to neuropathologic diagnosis. *Adv Anat Pathol* 22:50-58.
- Assanah M, Lochhead R, Ogden A, Bruce J, Goldman J, Canoll P (2006) Glial progenitors in adult white matter are driven to form malignant gliomas by platelet-derived growth factor-expressing retroviruses. *J Neurosci* 26:6781-6790.
- Baldewpersad Tewarie NM et al (2013) NADPp- dependent IDH1 R132 mutation and its relevance for glioma patient survival. *Med Hypotheses* 80:728–731.
- Bleeker FE, Atai NA, Lamba S, Jonker A, Rijkeboer D, Bosch KS, Tigchelaar W, Troost D, Vandertop WP, Bardelli A, Van Noorden CJ (2010) The prognostic IDH1 (R132) mutation is associated with reduced NADPp-dependent IDH activity in glioblastoma. *Acta Neuropathol* 119:487–494.
- Brennan CW et al (2013) The somatic genomic landscape of glioblastoma. *Cell* 155,462–477.
- Ceccarelli M et al (2016) Molecular Profiling Reveals Biologically Discrete Subsets and Pathways of Progression in Diffuse Glioma. *Cell* 164:550-563.
- Chen JR, Yao Y, Xu HZ, Qin ZY (2016) Isocitrate dehydrogenase (IDH)1/2 mutations as prognostic markers in patients with glioblastomas. *Medicine* 95:e2583.

- Chen L, Zhang Y, Yang J, Hagan JP, Li M (2013) Vertebrate animal models of glioma: understanding the mechanisms and developing new therapies. *Biochim Biophys Acta* 1836:158-165.
- Cheng Y, Ng HK, Ding M, Zhang SF, Pang JC and Lo KW (1999) Molecular analysis of microdissected de novo glioblastomas and paired astrocytic tumors. *J Neuropathol Exp Neurol* 58:120-128
- Dawson MR, Polito A, Levine JM, Reynolds R (2003) NG2-expressing glial progenitor cells: an abundant and widespread population of cycling cells in the adult rat CNS. *Mol Cell Neurosci* 24:476–488.
- Delgado-Lopez PD, Corrales-Garcia EM (2016) Survival in glioblastoma: a review on the impact of treatment modalities. *Clin Transl Oncol* 18:1062-1071.
- Di Rocco F, Carroll RS, Zhang J, Black PM (1998) Platelet-derived growth factor and its receptor expression in human oligodendrogliomas. *Neurosurgery* 42:341–346.
- Geisbrecht BV, Gould SJ (1999) The human PICD gene encodes a cytoplasmic and peroxisomal NADP(b)-dependent isocitrate dehydrogenase. *J Biol Chem* 274:30527–30533.
- Guo C et al (2011) Isocitrate dehydrogenase mutations in gliomas: mechanisms, biomarkers and therapeutic target. *Curr Opin Neurol* 24:648–652.
- Heldin CH, Westermark B (1999) Mechanism of action and in vivo role of platelet-derived growth factor. *Physiol Rev* 79:1283–1316.
- Heldin CH (2014) Targeting the PDGF signaling pathway in the treatment of non-malignant diseases. *J Neuroimmune Pharmacol* 9(2):69-79
- Hermanson M, Funa K, Hartman M, Claesson-Welsh L, Heldin CH, Westermark B, Nister M (1992) Platelet-derived growth factor and its receptors in human glioma tissue: expression

- of messenger RNA and protein suggests the presence of autocrine and paracrine loops. *Cancer Res* 52:3213–3219.
- Holland EC (2001) Gliomagenesis: genetic alterations and mouse models. *Nat Rev Genet* 2:120–129.
- Jacobs VL, Valdes PA, Hickey WF, De Leo JA (2011) Current review of in vivo GBM rodent models: emphasis on the CNS-1 tumour model. *ASN Neuro* 3(3):e00063.
- Koshland DE Jr, Walsh K, LaPorte DC (1985) Sensitivity of metabolic fluxes to covalent control. *Curr Top Cell Regul* 27:13–22.
- Krakstad C, Chekenya M (2010) Survival signalling and apoptosis resistance in glioblastomas: opportunities for targeted therapeutics. *Mol Cancer* 9: 135.
- Lee KS et al (2013) Immunohistochemical Classification of Primary and Secondary Glioblastomas. *Korean Journal of Pathology* 47(6):541-548.
- Margittai E, Banhegyi G (2008) Isocitrate dehydrogenase: a NADPH-generating enzyme in the lumen of the endoplasmic reticulum. *Arch Biochem Biophys* 471:184–190.
- Nagpal J et al (2006) Revisiting the role of p53 in primary and secondary glioblastomas. *Anticancer Res* 26:4633–9.
- Nazarenko I et al (2012) PDGF and PDGF receptors in glioma. *Ups J Med Sci* 117:99-112.
- Ohgaki H (2005) Genetic pathways to glioblastomas. *Neuropathology* 25:1-7.
- Ohgaki H, Kleihues P (2007) Genetic pathways to primary and secondary glioblastoma. *Am J Pathol* 170:1445-53.
- Ohgaki H, Kleihues P (2013) The definition of primary and secondary glioblastoma. *Clin Cancer Res* 19:764–72.

- Ostrom QT et al (2014) CBTRUS statistical report: primary brain and central nervous system tumors diagnosed in the United States in 2007-2011. *Neuro Oncol* 16 Suppl 4:iv1-63.
- Rong Y, Durden D, Meir EV, Brat D (2006) Pseudopalisading necrosis in glioblastoma: a familiar morphologic feature that links vascular pathology, hypoxia, and angiogenesis. *J Neuropathol Exp Neurol* 65(6):529-39.
- Seystahl K, Gramatzki D, Roth P, Weller M (2016) Pharmacotherapies for the treatment of glioblastoma - current evidence and perspectives. *Expert Opin Pharmacother* 17:1259-1270.
- Stupp R, Mason WP, van den Bent MJ, Weller M, Fisher B, Taphoorn MJ, Belanger K, Brandes AA, Marosi C, Bogdahn U, Curschmann J, Janzer RC, Ludwin SK, Gorlia T, Allgeier A, Lacombe D, Cairncross JG, Eisenhauer E, Mirimanoff RO (2005) Radiotherapy plus concomitant and adjuvant temozolomide for glioblastoma. *The New England Journal of Medicine* 352:987–996.
- Vogelstein B, Lane D and Levine AJ (2000) Surfing the p53 network. *Nature* 408:307-310.
- Westermarck B, Heldin CH, Nister M (1995) Platelet-derived growth factor in human glioma. *Glia* 15:257–263.
- Xu H, Zong H, Ma C, Ming X, Shang M, Li K, He X, Du H, Cao L (2017) Epidermal growth factor receptor in glioblastoma. *Oncol. Lett* 14:512–516.